Mansoura Veterinary Medical Journal

Manuscript 1249

Impact of ellagic acid loaded zinc nanoparticles on cardiac and hepatic tissue on Type 1 diabetic rats

Gehad R. M. Elsayed

Afaf D. Abdelmagid

Hatem B. Huseiny

Ahmed Fotoh

See next page for additional authors

Follow this and additional works at: https://mvmj.researchcommons.org/home

Impact of ellagic acid loaded zinc nanoparticles on cardiac and hepatic tissue on Type 1 diabetic rats

Authors

Gehad R. M. Elsayed, Afaf D. Abdelmagid, Hatem B. Huseiny, Ahmed Fotoh, and Faten E. Shoker

ORIGINAL ARTICLE

Impact of Ellagic Acid-loaded Zinc Nanoparticles on Cardiac and Hepatic Tissues on Type 1 Diabetic Rats

Faten E. Shoker [1,*], Gehad R.M. Elsayed [1], Afaf D. Abdelmagid [2], Hatem B. Huseiny [3], Ahmed Fotouh [4]

[1] Department of Biochemistry, Faculty of Veterinary Medicine, Mansoura University, Mansoura, Egypt
[2] Department of Biochemistry, Faculty of Veterinary Medicine, Benha University, Benha, Egypt
[3] Department of Anatomy and Embryology, Faculty of Veterinary Medicine, Benha University, Benha, Egypt
[4] Department of Pathology and Clinical Pathology, Faculty of Veterinary Medicine, New Valley University, El-Kharga, Egypt

Abstract

BACKGROUND: Biochemical, molecular, and histopathological alterations are the most noticeable clinical and pathological characteristics attributed to diabetes mellitus. An imbalance in these parameters increases the risk of developing complications. Therefore, the main objective of this study was to determine the cardiac and hepatic protective effects of ellagic acid-loaded zinc nanoparticles (EA-ZnNPs) on diabetes, which were evaluated biochemically, molecularly, and histopathologically.

METHODS: Four groups of 40 adult male rats were established in this study. The groups were subsequently classified as control, streptozotocin (STZ) diabetic, STZ treated with EA-ZnNPs, and STZ treated with insulin. After 6 weeks of treatment, blood, heart, and liver tissue samples were obtained, and biochemical, molecular, and histopathological examination were performed.

RESULTS: Treatment with EA-ZnNPs or insulin had significant consequences, as evidenced by the restoration of cardiac and hepatic damage, as well as a substantial reduction in the serum levels of heart and liver-related parameters, such as triglycerides, serum cholesterol, creatine kinase MB isoenzyme, lactate dehydrogenase, alanine aminotransferase, aspartate aminotransferase, cardiac and hepatic malondialdehyde, glutathione peroxidase, catalase, and inflammatory indices. Additionally, there were notable histological changes in the hepatic histoarchitecture of diabetic rats treated with EA-ZnNPs.

CONCLUSION: EA-ZnNPs could serve to preserve the liver and cardiac tissue in rats with diabetes.

Keywords: Diabetes, Ellagic acid loaded zinc nanoparticles, Heart, Liver, Streptozotocin

1. Introduction

Diabetes mellitus (DM) is a serious metabolic disorder characterized by high blood glucose levels caused by impaired insulin production or consumption. It is now considered a global epidemic that affects millions of people worldwide. About 463 million people between the ages of 20 and 79 had DM in 2019 Rawshani, Sattar [1].

Reactive oxygen species (ROS), which are produced by hyperglycemia, cause damage to the cells in many ways. Cell damage eventually leads to

Abbreviations: ALT, alanine aminotransferase; AST, aspartate aminotransferase; CK-MB, creatine kinase-MB; COX-2, cyclooxygenase-2; DC, diabetic complication; DM, diabetes mellitus; EA, ellagic acid; EA-ZnNPs, ellagic acid loaded zinc nanoparticles; GPX, gutathione peroxidase; HMGCoAR, β-hydroxy β-methylglutaryl-CoA reductase; IkB, inhibitor of kappa B; IL-10, interleukin 10; IL-6, interleukin 6; LDH, lactate dehydrogenase; MDA, malondialdehyde; NADPH, the nicotinamide adenine dinucleotide phosphate; NF-κB, nuclear factor kappa-light-chain-enhancer of activated B cells; ROS, reactive oxygen species; SOD, superoxide dismutase; STZ, streptozotocin; T1DM, Type 1 diabetes mellitus; TC, serum total cholesterol; TGs, triglycerides; TNF-α, tumor necrosis factor-alpha; Zn, zinc; $ZnCl_2$, zinc chloride.

Received 11 March 2024; revised 3 September 2024; accepted 4 September 2024.
Available online 25 October 2024

* Corresponding author at: Department of Biochemistry, Faculty of Veterinary Medicine, Mansoura University, 35516, Egypt.
E-mail address: fatenelkenanyshoker644@Gmail.com (F.E. Shoker).

https://doi.org/10.35943/2682-2512.1249
2682-2512/© 2024, The author. Published by Faculty of Veterinary Medicine Mansoura University. This is an open access article under the CC BY 4.0 Licence (https://creativecommons.org/licenses/by/4.0/).

secondary complications of DM. Thus, oxidative stress is one of the main causes of cardiovascular disease in individuals with DM. An intense association has been found between DM and elevated oxidative stress, as evidenced by the increased accumulation of lipid peroxidase in the plasma of patients with DM [2]. In DM, macrovascular complications result from damage to large blood vessels and are mainly heart problems such as myocardial infarction, ischemic heart disease, and early atherosclerosis [3]. Death rates for heart disease and the risk of stroke are ~2−4 times higher among adults with diabetes than among those without DM [4]. Cardiac dysfunction caused by cardio-toxic agents such as streptozotocin (STZ) may lead to heart failure, myocardial ischemia, arrhythmias, hypertension, myocarditis, pericarditis, and thromboembolism [5].

DM in a long-term state affects the liver's ability to function normally and can lead to conditions like inflammation and a fatty liver [6]. Hyperglycemia can lead to hepatocyte mitochondrial dysfunction in diabetic animals and humans, as well as oxidative stress, oxidative phosphorylation reduction, and ultrastructural abnormalities [7]. Another study [8] discovered that in type 1 diabetes in rats, hyperglycemia can result in hydroxyl radical-induced hepatocyte apoptosis.

Subcutaneous insulin therapy is the main treatment option for DM. Nevertheless, it does not always offer the metabolic control required to prevent problems related to the disease. Additionally, this route of drug administration is attributed to low patient comfort owing to the risk of pain, distress, and local inflammation or infections [9]. In addition, several side effects, including insulin resistance (a situation in which cells are ineffective in their utilization of insulin occasionally combined with an absolute insulin inadequacy), brain atrophy, anorexia nervosa, and fatty liver, have been reported in patients on lifelong medication with insulin therapy and allopathic diabetic drugs [10]. To address the above-mentioned problems, our research is focused on nanotechnology, which is a promising approach to increase therapeutic efficacy and reduce adverse effects. Nanoparticles have been suggested to allow the drug to be administered via less invasive routes other than injection, such as oral administration. In this regard, nanomedicine, an organic-inorganic nanoformulation, has recently been used for the treatment of diabetic complications (DC). This formula has led to an increase in the use of inorganic nanoparticles, with natural compounds being screened for the treatment of several major diseases, including cancer, DM, and cardiovascular, inflammatory, and microbial diseases. Furthermore, metal-based drug delivery systems have been studied as drug delivery systems due to their optical, catalytic, magnetic behavior, ease of surface modification, and large surface area [11].

Plant extracts are intriguing therapeutic options because of their specific advantages, such as anti-inflammatory, antioxidant, and insulin-sensitizing capabilities in controlling hyperglycemia. Antioxidants derived from medicinal plants have received increased interest as free radical scavengers because they protect against ROS- oxidative stress and damage [12]. These make them favorable leads in the discovery of novel drugs. Ellagic acid (EA) is an organic hetero-tetra-cyclic molecule with the chemical formula C_{14} H_6 O_8 and planar phenolic lactone properties. Numerous fruits and vegetables, including pomegranates, cranberries, strawberries, and raspberries contain it. It functions as a naturally occurring polyphenol antioxidant, a class of anti-cancer medications [13]. EA possesses wound-healing properties, antibacterial and antiviral effects, and is added to drug delivery systems, such as silver nanoparticles [14] and zinc-layered hydroxides [15]. EA is associated with anti-DM, anti-inflammatory, and neuroprophylactic characteristics [16]. However, clinical applications of this polyphenol have been hampered and prevented by its poor water solubility and pharmacokinetic profile (limited absorption rate and low penetration, and eliminated quickly from the body [17].

In the past few years, a large number of studies have been reported on engineering nanoparticulate systems loaded with ellagic acid that exhibit superior biological activities over conventional therapeutics. As an example, the research study carried out by Harakeh *et al.* stated that the antidiabetic activity of ellagic acid nanoparticles is mediated by the suppression of beta-cell death and the enhancement of insulin production [18]. In another study, EA loaded onto chitosan nanoparticles coated with a nonionic surfactant (Tween 80) demonstrated a potential effect against breast cancer, studied *in vitro* and *in vivo* [19]. A nanoparticulate formulation was developed for sustained-release with antioxidant EA as a possible prophylaxis when administered orally [20]. In both a yeast cell culture model and a cell-free system, EA-loaded nanoparticles exhibited greater free radical scavenging efficacy.

Zinc (Zn) is found in all human tissues, organs, bodily fluids, and secretions. It is an element that the body needs for normal development. More than 300 enzymes contain Zn, making it a necessary component of many enzymes engaged in significant

metabolic pathways in the body [21]. Zn inhibits glucagon secretion, which reduces gluconeogenesis and glycogenolysis, and also has an impact on insulin production, secretion, storage, and structural integrity [22], which means it can control and extend insulin's hypoglycemic effect. According to Qi *et al.* [23], Zn is also a cofactor of enzymes that break down lipids and proteins and a component of several enzymes that metabolize glucose.

To the best of our knowledge, this is the first study to evaluate the therapeutic efficacy of newly synthesized ellagic acid-loaded zinc nanoparticles (EA-ZnNPs) in albino rats to determine their protective effects in the heart and liver against STZ induced DM. Serum biochemical markers associated with the heart and liver were assessed. The livers of rats were histopathologically examined as part of this investigation.

2. Material and methods

2.1. Materials

The Department of Spectroscopy at the National Research Center in Dokki, Giza, Egypt, developed EA-ZnNPs (29 nm). STZ was purchased from Sigma Chemicals Co. (St. Louis, MO, USA). Alfa Aesar supplied the anhydrous, 98+% zinc chloride ($ZnCl_2$). Lantus Solostar, Sano-fi-Aventis, Germany, supplied long-acting insulin. FineTest Autocoding Premium Blood Glucose Meter (model: IGM-0017B). The aqueous solutions of EA-ZnNPs were all prepared with distilled water.

2.2. Methods

2.2.1. Extraction of ellagic acid

EA was extracted from the pomegranate peel powder (*Punica granatum*), and the pomegranate peel was purchased from the Egyptian market. According to Lu and Yuan [24], the crushed pomegranate peel was immersed in 60 % aqueous ethanol and stirred over a hot plate. The tannin that results from this extract was filtrated and hydrolyzed by 5 % H_2SO_4 for 5 h and left overnight. The dark brown crude precipitate EA was collected, dissolved in ethanol, filtered, and left to dry in the oven at 50 °C.

2.2.2. Biosynthesis and characterization of EA-ZnNPs

ZnNPs were synthesized according to Moreno-Álvarez *et al.* [25]. In brief, 2.0 ml of $ZnCl_2$ (20 mM) was mixed with 46.0 ml of double-distilled water at room temperature using magnetic stirring. EA solution and ZnNPs were combined in a 9:1 ratio. After adding EA, the pH was adjusted to 11.0 with 1.0 M NaOH. The reaction was then sustained at room temperature for 30 min, and the nanoparticles were condensed and purified by centrifugation at 15,000 r.p.m. for 10 min, followed by three washes with double-distilled water.

The prepared sample is analyzed utilizing the KBr disc technique on a Fourier transformer infrared spectrometer (Nexus 670 FTIR, USA) in the 400−4000 cm^{-1} range. The Ultraviolet visible spectrum (UV/VIS) is measured in the wavelength range of 190−900 nm using the JASCO (Japan Spectroscopic Company, Japan) double beam spectrophotometer V-570 UV/VIS/NIR to manifest particle size and distribution.

Transmission electron microscopy (TEM) is used to examine the size, nature, and shape of newly synthesized EA-ZnNPs. The nanoparticle solution is sonicated for 5 min to improve particle dispersion and prevent particle aggregation on the copper grid. Following that, a TEM sample of EA-ZnNPs is generated by adding a drop of nanoparticle solution to carbon-coated copper grids and allowing the water to evaporate. The morphology of the prepared solution and the particle size are evaluated using a high-resolution transmission electron microscope (HR-TEM; JEOL, JEM2100, Electron Microscope, Japan).

2.2.3. Acute toxicity study

EA-ZnNPs (dissolved in distilled water) and shacked before being administered by gavage at doses of 0, 1, 10, 20, 100, 300, and 500 mg/kg body weight to various groups, which had five animals each. Following treatment, the animals were monitored continuously for 1 h, then for 4 h, and thereafter over a period of 24 h to look for behavioral modifications, toxicity, and/or death symptoms, as well as the latency of death. For 14 days, animals were provided food and water, and their daily food intake, water consumption, body weight, death, and visual changes were all recorded. The median lethal dose (LD50), which caused death in 50 % of the population of the experimental animals, was determined according to the method of Litchfield and Wilcoxon [26].

2.2.4. Selection of therapeutic dose

The effective dose (20 mg/kg) was fixed based on a toxicity study for EA-ZnNPs and the antioxidant activity of orally administered ellagic acid nanoparticles [27].

2.2.5. Experimental animals

At the start of the experiment, 40 male albino rats, weighing between 180 and 200 g and 5−6 weeks old,

were housed in conventional laboratory settings (25 ± 10 C, 12/12 h cycle of light and dark). Animals were purchased from the National Research Center's Animal House Colony in Giza, Egypt. As part of their acclimatization procedure, the rats received regular access to food and clean water for 2 weeks before the beginning of the experiment. After the adaptation phase, the rats were randomly distributed into four groups.

2.2.6. Diabetes induction and evaluation

Intraperitoneal injection (i.p.) of STZ (dissolved in citrate buffer 0.1 mol/l, pH 4.2) at 60 mg/kg b.wt. for three consecutive days developed type 1 diabeteis mellitus [28]. After 24 h of STZ injection and an overnight fast, blood was taken from the tail vein and tested using the FineTest Autocoding Premium Blood Glucose Meter. Animals with an FBG level higher than 250 mg/dl were selected for the diabetic groups. To guarantee DC onset, the diabetic rats were maintained for 2 weeks following the induction of DM.

2.2.7. Animal grouping

The animals were distributed into four groups randomly, each with 10 rats.

Group 1: received 1 ml of distilled water per 100 g bwt per day by oral gavage and served as a negative control group (−ve). The remaining 30 rats were distributed into three equal groups after receiving treatment with STZ to induce DM.

Group 2: injected i.p. with STZ in a dose of 60 mg/kg bwt for 3 consecutive days and served as untreated diabetic group.

Group 3: diabetic rats treated with EA-ZnNPs: 2 weeks after 2 weeks of administration of STZ, they were given 20 mg/kg b.wt of EA-ZnNPs orally every day for 6 weeks.

Group 4: diabetic rats treated with insulin: the animals were given STZ, and then, after 2 weeks, they were given insulin (2 units per rat, i.p.) once a day for 6 weeks [29].

N.B.: During the experimental period, the dosage was adjusted every week according to any change in body weight to maintain a similar dose per kg of body weight per rat over the entire period of study for each group.

2.2.8. Blood and tissue samples collection

After overnight fasting, samples of blood were collected from a wake rats through Retro-orbital Venus plexus at the end of the experiment in dry, clean, screw-capped tubes, and serum was separated by centrifugation at 3000 r.p.m. for 15 min. The clean, clear serum was separated by an automatic pipette, received in a dry, sterile sample tube, and used directly for the biochemical determination of serum total cholesterol (TC), triglycerides (TGs), creatine kinase-MB (CK-MB), lactate dehydrogenase (LDH), alanine aminotransferase (ALT), and aspartate aminotransferase (AST). The animals were sacrificed by cervical dislocation after using ether inhalation anesthesia, their hearts and livers were quickly removed and kept at −80 °C for RT-PCR and molecular studies. Furthermore, sections of each group's heart and liver were fixed for histopathological analysis after being cleaned in normal saline and isolated in 10 % formalin.

2.2.9. Assessment of biochemical parameters

The serum parameters, like serum TC was estimated using the enzymatic colorimetric method [30] using the Spinreact kit (Catalogue No. 41020, Sant Esteva de Bas, Girona, Spain). TGs were analyzed based on colorimetric method according to Fossati and Prinicip [31], using the Spinreact kit (Catalogue No. 41030, Sant Esteva de Bas, Girona, Spain). Serum aminotransferases (AST and ALT) enzyme activity was measured based on kinetic reactions method [32], using Human Diagnostics kit (Catalogue No for AST. 12021 and for ALT. 12022, Wiesbaden, Germany) [33]. Used the enzymatic method to estimate LDH using a Diamond kit (Diamond Diagnostics, Cairo, Egypt). All tests was performed using a spectrophotometer (Photometer 5010 Boehringer Mannheim GmbH, Germany). Serum CK-MB was determined by ELISA using a commercial kit (Biodiagnostic Co., Cairo, Egypt) by Stat Fax 4700 ELISA reader (Awareness Technology, Palm city, USA).

2.2.10. Preparation and evaluation of tissue malondialdehyde (MDA) concentration, and antioxidant enzymes

Briefly, heart and liver tissues were cut, weighed, and minced into small pieces and homogenized with a glass homogenizer in 9 volumes of ice-cold 0.05 mM potassium phosphate buffer (pH 7.4) to make 10 % homogenates. The homogenates were centrifuged at 6000 rpm for 15 min at 4 °C, and the resultant supernatant was used for the determination of the following parameters:

The MDA concentration was determined colorimetrically [34]. The principle measurement of malondialdehyde depends on the determination of thiobarbituric acid reactive substance content (TBARS). Thiobarbituric acid reacts with malondialdehyde in an acidic medium at a temperature of 100 °C for 15 min to form thiobarbituric acid-reactive products. The absorbance of the resultant color product can be measured at 534 nm, using a

commercial kit (Bio-diagnostic Co., Cairo, Egypt) in a plate reader (SPECTRO star Nanodrop, BMG LABTECH, Offenburg, Germany). The activity of glutathione peroxidase (GPx) was estimated by UV method [35] in SPECTRO star Nanodrop, using a commercial kit (Bio-diagnostic Co., Cairo, Egypt). Catalase enzyme activity was determined by colorimetric method [36], using a commercial kit (Bio-diagnostic Co., Cairo, Egypt) in SPECTRO star Nanodrop.

2.2.11. Gene expression analysis

(a) RNA extraction: The RNeasy Kit (Catalogue No. 74104; Qiagen, Hilden, Germany) was used to extract the total RNA from the heart and liver tissues of male rats, as 30 mg from the tissue sample was added to 600 µl RNA Lysis Tissue (RLT) buffer (10 µl β-Mercaptoethanol/ml Buffer RLT). Tubes were placed into the adaptor sets, which are fixed into the clamps of the Qiagen tissue lyser for the homogenization of samples. In 2 min, high-speed (30 Hz) shaking step disruption was done. To the cleared lysate, 70 % ethanol one volume was added, and the steps were done according to the total RNA purification from animal tissues protocol of the RNeasy Mini Kit instructions.
(b) Oligonucleotide Primers: Primers used were supplied from Metabion (Germany) are listed in Table 1.
(c) SYBR green (a dsDNA binding dye) rt-PCR: Primers were used in a 25 µl reaction containing 12.5 µl from the 2× QuantiTect SYBR Green PCR Master Mix (Qiagen, Germany, GmbH), 0.25 µl from RevertAid Reverse Transcriptase (200 U/µl) (Thermo Fisher) Catalogue number: EP044, 0.5 µl of each primer of 20 pmol concentration, 8.25 µl of water, and 3 µl of RNA template. The reaction was carried out in a Stratagene MX3005P real-time PCR machine.
(d) Analysis of RT-PCR results: By the Stratagene MX3005P software, amplification curves and CT values were determined. The CT of each sample was compared with that of the positive control group to estimate the variation of gene.

Expression on the RNA of the different samples, according to the 'ΔΔCt' method stated by Yuan *et al.* [37], using the following ratio: ($2^{-\Delta\Delta ct}$).

Whereas ΔΔct = Δct reference − Δct target

Δct target = CT control − CT treatment and Δct reference = CT control- CT treatment

E: efficiency of amplification.

2.2.12. Histopathological screening

According to [41], liver tissue samples from all animals were taken out, cleansed with saline, preserved in 10 % buffered neutral formalin, dried using blocks of paraffin wax, and inspected under a microscope. Utilizing a semi-quantitative scoring system, the slides were assessed by a pathologist, and liver tissue samples for different lesions were scored.

2.2.13. Statistical analysis

The data was reported according to its qualitative or quantitative nature. Qualitative data was evaluated as percentages, whereas quantitative data was provided as a mean with a standard error of the mean (S.E.). The one-way ANOVA was used to determine any statistical differences between the groups, followed by Tukey's multiple comparisons test. A *P* value of less than 0.05 was considered significant. The statistical evaluation of the data was conducted using GraphPad Prism (GraphPad Software, San Diego, California, USA).

3. Results

3.1. Characterization of EA-ZnNPs

FT-IR spectroscopy was performed to identify the functional groups of the synthesized EA-ZnNPs. The IR absorbance spectra of the samples were obtained in the range of 4000−400 cm^{-1}. Fig. 1 shows the FT-IR spectrum of EA-ZnNPs. The band at 3263 is a characteristic band attributed to the high concentration of the hydroxyl group (O−H), a medium band at 1636 cm^{-1} to the stretching vibration of the C=C bond, the band assigned to 1735 cm^{-1} was observed due to the lactone ring, the band is assigned to 758 cm^{-1} to CH aromatic c bending, and

Table 1. Oligonucleotide primers in SYBR Green real time PCR.

Reference	Primer sequence (5′-3′)	Gene
[38]	TCCTCCTGAGCGCAAGTACTCT GCTCAGTAACAGTCCGCCTAGAA	Rat ß. Actin
[39]	GCGGCTGAGGCGCTGTCAT CGCCTTGTAGACACCTTGGTCTTGG	IL10
[40]	GCAAACCTGGGAATACTTCATGTGACTAAG ATAGGCAAGGTCAGAATGCACCAGAAGTCC	NF-κB

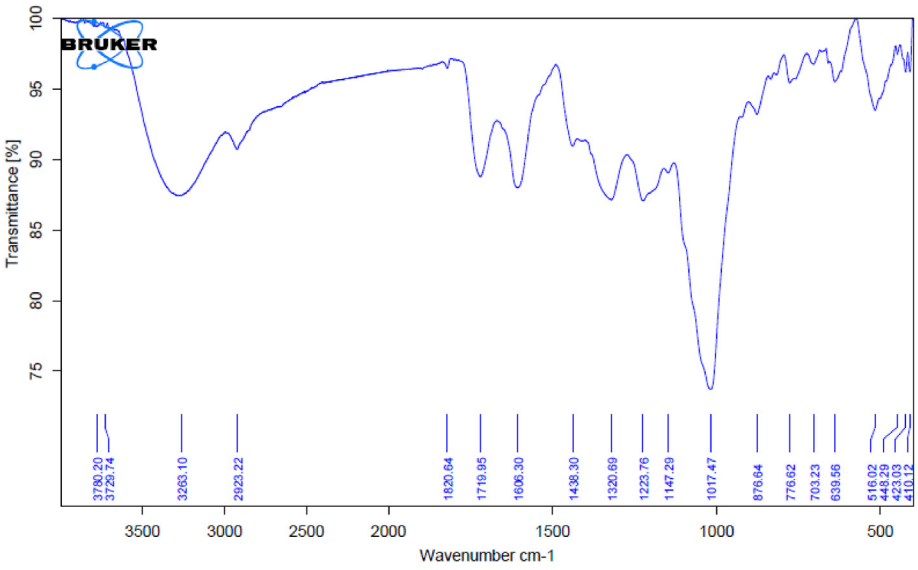

Fig. 1. The FT-IR spectrum of ellagic acid loaded zinc nanoparticles.

the peak at 1017 cm^{-1} to the ester linkage of the expansion of C–O.

In Fig. 2. The UV-vis spectra of EA-ZnNPs revealed a major peak at 278 assigned to the surface plasmon resonance of the nanoparticles and a narrow peak at 372 nm. Electron microscopy transmittance graphs of EA-ZnNPs coated are shown in Fig. 3. It was observed that the size of the nanoparticles was an average of 29.1 nm and appeared as spherical clusters in shape.

3.2. Acute toxicity

No signs of toxicity or death were observed after oral administration of the EA-ZnNPs up to the dose of 500 mg/kg BW.

3.3. Biochemical results

3.3.1. Serum TC and TGs levels

I.p. injection of STZ markedly elevated the mean values of serum concentrations of TC and TGs in the diabetic group when compared with the control group. In contrast to the diabetic group, treatment with EA-ZnNPs and insulin significantly reduced the increase in blood TC and TGs. Furthermore, treatment with EA-ZnNPs and insulin resulted in no significant difference in TC levels but a significant difference in TG levels when compared with the control group (Fig. 4).

3.3.2. Serum CK-MB and LDH activities

The mean values of CK-MB and LDH activities of diabetic rats were significantly increased when

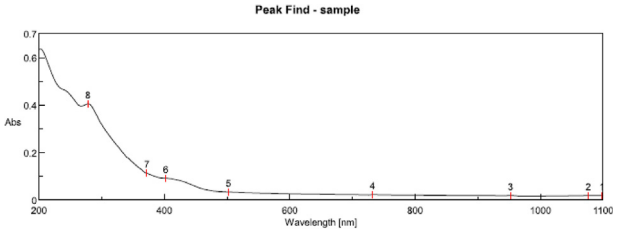

Fig. 2. The Ultraviolet-visible- spectra of ellagic acid loaded zinc nanoparticles.

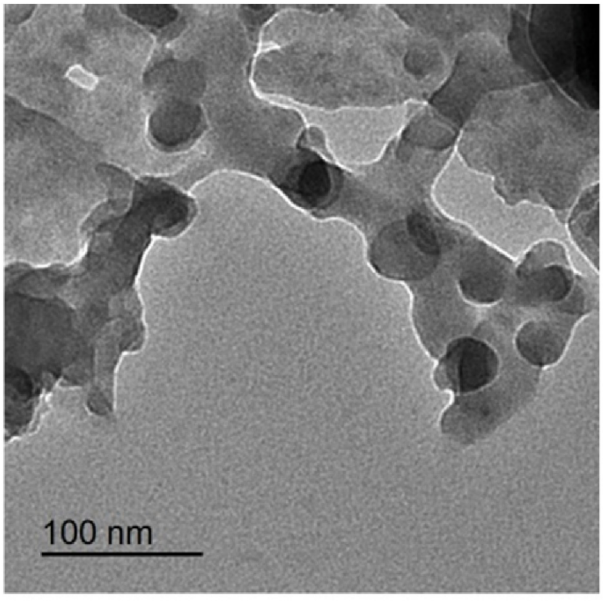

Fig. 3. TEM image of ellagic acid loaded zinc nanoparticles.

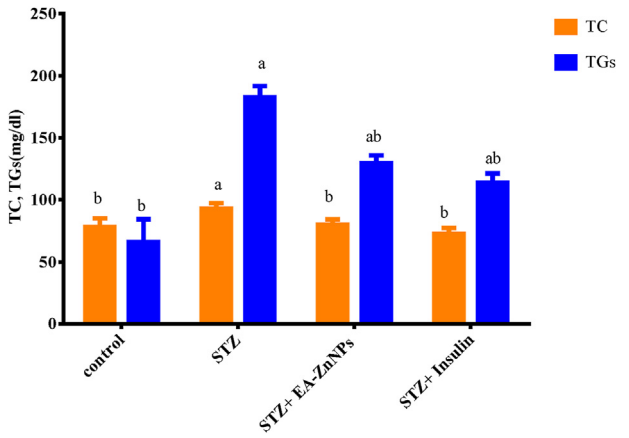

Fig. 4. Effect of ellagic acid loaded zinc nanoparticles on serum total cholesterol and triglycerides levels in diabetic rats. Data represents Mean ± SE. a Significantly different compared with control group, b Significantly different compared with streptozotocin group at (P < 0.05).

compared with the control group. However, treatment with EA-ZnNPs and insulin exhibited a significant decrease in mean values of CK-MB and LDH activities. Furthermore, treatment with EA-ZnNPs and insulin showed a significant difference in CK-MB and LDH activities when compared with control-treated groups (Fig. 5).

3.3.3. Serum ALT and AST activities

I.p. injection of STZ markedly elevated the mean values of liver enzymes ALT and AST activities when compared with the control group. However, treatment with EA-ZnNPs and insulin substantially reduced the rise of ALT and AST activities. Additionally, treatment with EA-ZnNPs and insulin showed a significant difference in ALT and AST activities when compared with the control group (Fig. 6).

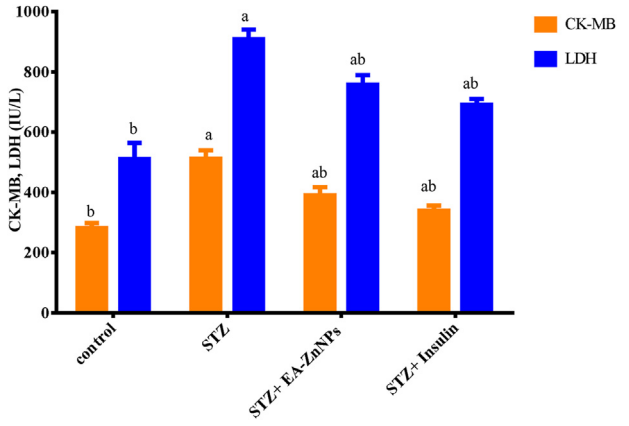

Fig. 5. Effect of ellagic acid loaded zinc nanoparticles on serum CK-MB and LDH activities in diabetic rats. Data represents Mean ± SE. a Significantly different compared with control group, b Significantly different compared with streptozotocin group at (P < 0.05).

3.4. Oxidative stress biomarkers in heart and liver tissues

Diabetic rats induced by STZ exhibited a substantial rise in MDA levels in the heart and liver tissues when compared with the control group. The treatment with EA-ZnNPs and insulin substantially reduced levels of MDA in heart and liver tissues when compared with diabetic rats. Additionally, treatment with EA-ZnNPs and insulin showed no significant difference in MDA levels when compared with the control group (Fig. 7). As regards GPX and catalase, there was a marked decrease in GPX and catalase activity levels in the heart and liver tissues when compared with control rats. GPX and catalase activities in STZ-induced diabetic rats treated with EA-ZnNPs and insulin showed a significant increase when compared with diabetic rats. Moreover, treatment with EA-ZnNPs and insulin showed a significant difference in heart and liver GPX when compared with the control group. Furthermore, catalase activities in EA-ZnNPs and insulin-treated groups showed no significant difference in liver with a significant difference in heart when compared with the control group (Figs 8 and 9).

3.5. The effects of EA-ZnNPs on molecular genes in heart and liver tissues

The acquired data in Figs 10 and 11 demonstrated that diabetic rats (group 2) exhibited significant

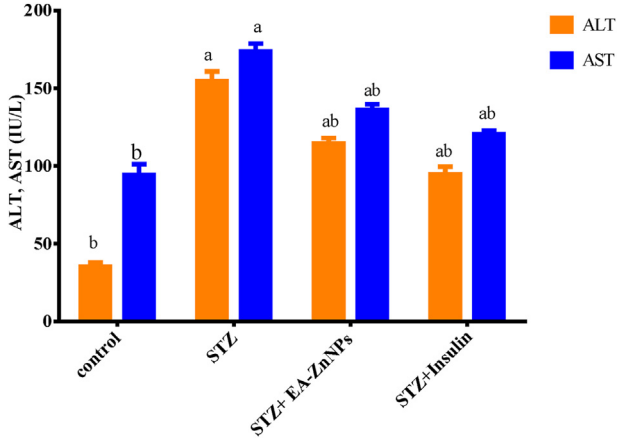

Fig. 6. Effect of ellagic acid loaded zinc nanoparticles on serum alanine aminotransferase and aspartate aminotransferase activities in diabetic rats. Data represents Mean ± SE. a Significantly different compared with control group, b Significantly different compared with streptozotocin group at (P < 0.05).

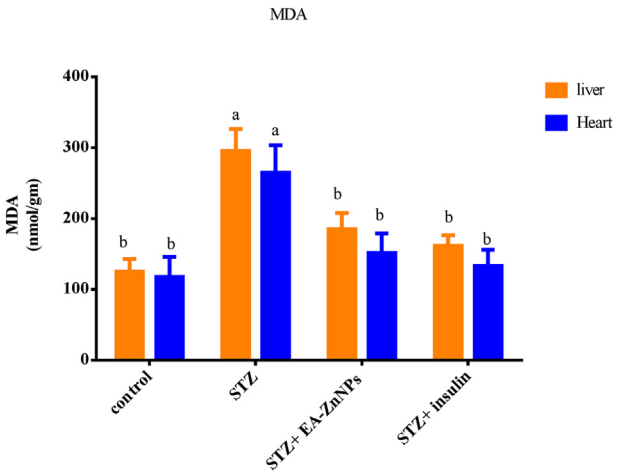

Fig. 7. Effect of ellagic acid loaded zinc nanoparticles on hepatic and cardiac levels of L-malondialdehyde in diabetic rats. Data represents Mean ± SE. a Significantly different compared with the control group, b Significantly different compared with streptozotocin group at (P < 0.05).

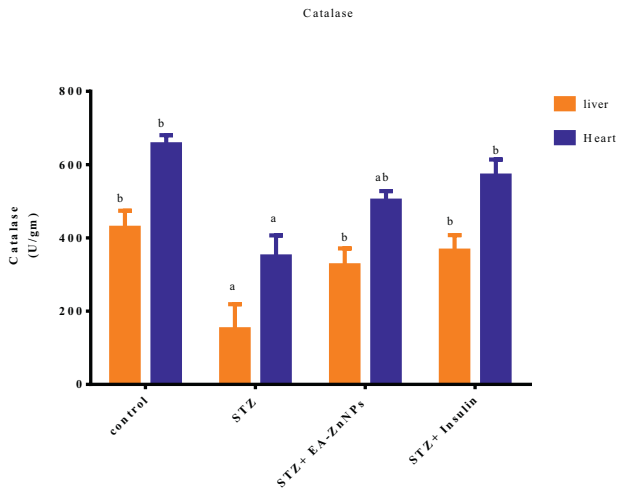

Fig. 9. Effect of ellagic acid loaded zinc nanoparticles on hepatic and cardiac catalase activities in diabetic rats. Data represents Meant ± SE. a Significantly different compared with control group, b Significantly different compared with streptozotocin group at (P < 0.05).

upregulation of nuclear factor kappa-light-chain-enhancer of activated B cells (NF-kB) and significant downregulation in interleukin 10 (IL-10) gene expression in comparison to the normal control group. When STZ-induced diabetic rats were treated with EA-ZnNPs and insulin, there was an apparent rise in the expression of the IL-10 gene and a significant downregulation in NF-kB gene expression in comparison to the diabetic group. However, treatment with EA-ZnNPs showed a significant difference in heart and liver NF-kB when compared with the control group. Also, NF-kB gene expression in insulin-treated groups showed no significant difference in the heart with a significant difference in liver. While IL-10 gene expression in insulin-treated groups showed no significant difference in heart and liver, with a significant difference in the EA-ZnNPs-treated group when compared with the control group.

3.6. Histopathological studies of hepatic tissues in STZ-diabetic rats after administration of EA-ZnNPs

The photomicrograph of the control group's liver during the histological analysis reveals adequate liver structure; each lobe is divided into numerous classic lobules that contain sinusoids and plates of

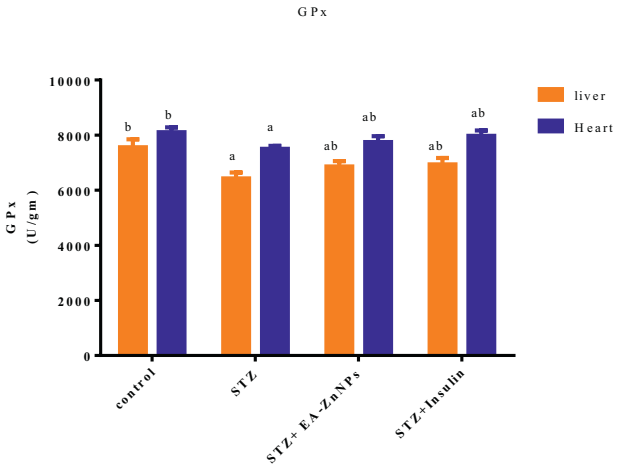

Fig. 8. Effect of ellagic acid loaded zinc nanoparticles on hepatic and cardiac glutathione peroxidase activities in diabetic rats. Data represents Mean ± SI,. a Significantly different compared with control group, b Significantly different compared to streptozotocin group at (P < 0.05).

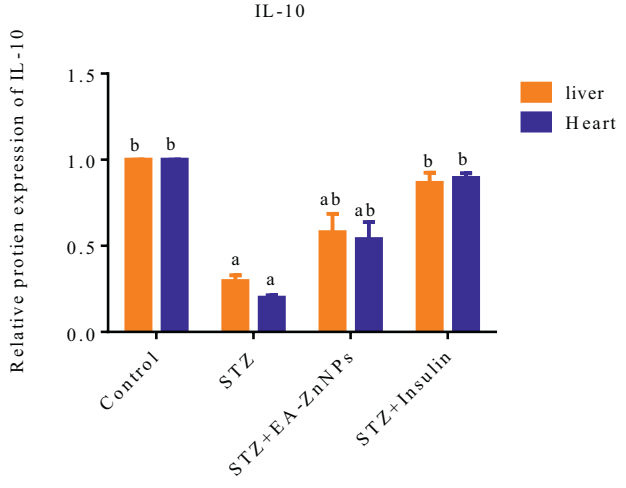

Fig. 10. Real-time PCR analysis of mRNA expression level of interleukin 10 in diabetic rats. Data represents Mean ± SE. a Significantly different compared with control group, b Significantly different compared with streptozotocin group at (P < 0.05).

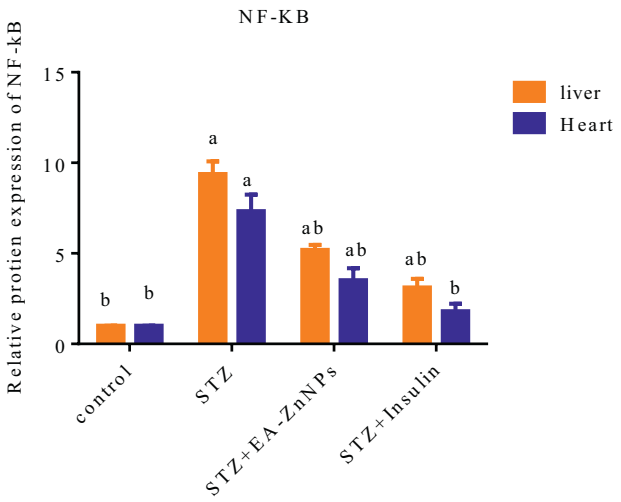

Fig. 11. Real-time PCR analysis of mRNA expression level of nuclear factor kappa-light-chain-enhancer of activated B cells in diabetic rats. Data represents Mean ± SE a Significantly different compared with control group, b Significantly different compared with streptozotocin group at (P < 0.05).

hepatocytes radially distributed around the central vein (Fig. 12a).

Histopathological examination of diabetic rats' liver shows an obvious sign of hepatic alterations; these include congested central vein with sinusoidal dilatation (Fig. 12b). Mild vacuolar degeneration around the central veins (Fig. 12c). Focal hepatic necrosis with mononuclear inflammatory cell infiltration (Fig. 12d). Diabetic rats treated with Zn NPs and insulin showed amelioration in most pathologic lesions (Fig. 12e-f).

Treatment with EA-ZnNPs substantially lowered the elevation of vacuolar degeneration grades by 35.3 %; also, insulin-treated groups showed a 67.6 % decrease in vacuolar degeneration grades (Fig. 13). Treatment with EA-ZnNPs substantially lowered the elevation of vascular and sinusoidal congestion

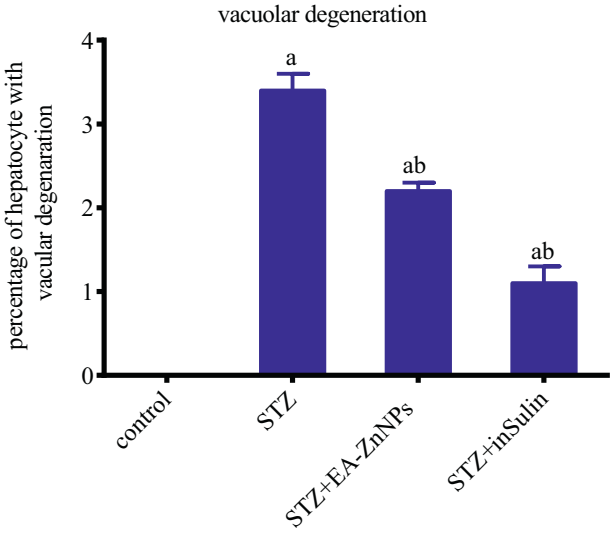

Fig. 13. Effect of ellagic acid loaded zinc nanoparticles on grades of vacuolar degeneration in liver specimen a. Significantly different compared with control group, b Significantly different compared with streptozotocin group at (P < 0.05).

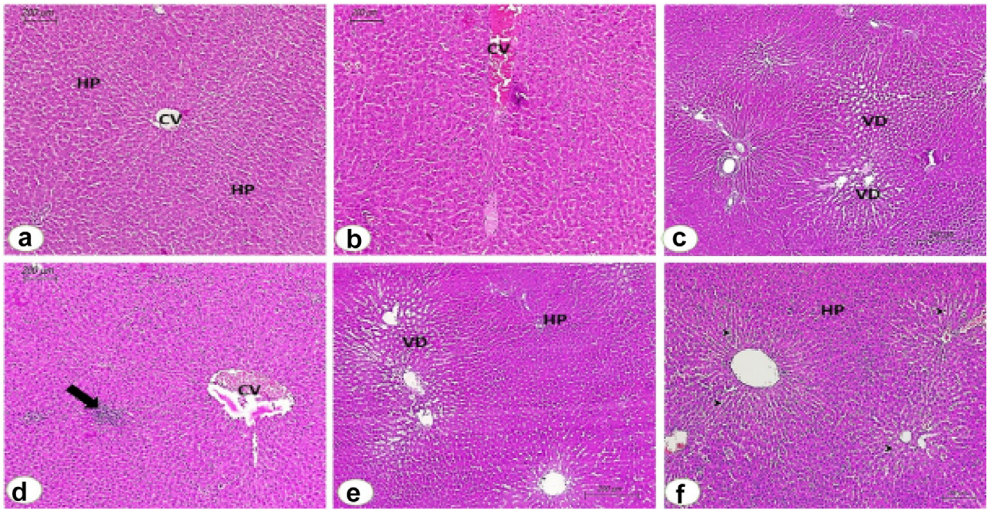

Fig. 12. Liver from rat (3 months); (a) (−ve control group) showing normal hepatic parenchyma (HP) divided into lobes Every lobe is separated into many typical lobules around central vien (CV) (H and E, scale bar: 200 μm). (b) Nontreated diabetic group showing; normal hepatic parenchyma with severely congested central vien (CV) (H and E, scale bar: 200 μm); (c) Nontreated diabetic group with vacuolar degeneration (VD) of hepatic parenchyma especially around central veins. (H and E, scale bar: 200 μm); (d) Nontreated diabetic group with focal aggregation of inflammatory cells (arrow) and congested central vien (CV) (H and E, scale bar: 200 μm). (e) EA-Zn NPs treated group showing mild vacuolar degeneration (VD) of hepatic parenchyma (HP) (H and E, scale bar: 200 μm). (f) Insulin treated group showing mild sinosoidal congestion (arrow heads) of hepatic parenchyma (HP) (H and E, scale bar: 200 μm).

grades by 40.0 %. Additionally, insulin-treated groups showed a 58.7 % grade of vascular and sinusoidal congestion (Fig. 14). Treatment with EA-ZnNPs substantially lowered the elevation of mononuclear cellular infiltration grades by 50.8 %. Furthermore, insulin-treated groups showed a 62.6 % decrease in grades of mononuclear cellular infiltration (Fig. 15). Additionally, both the EA-ZnNPs and insulin-treated group showed a 45.9–54.7 % decrease in the injury of blood vessel intima in liver grades, respectively (Fig. 16).

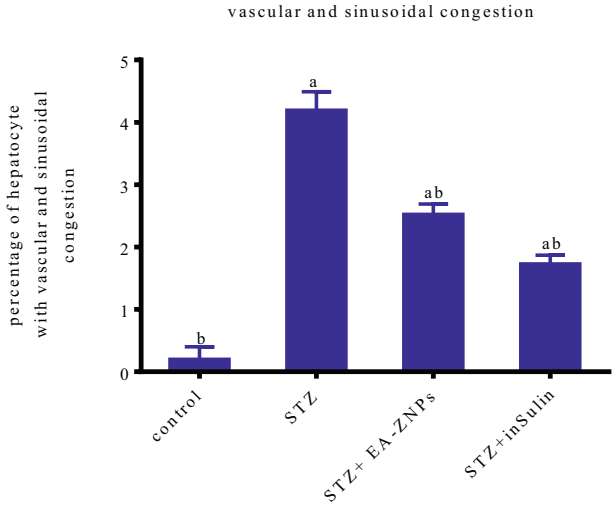

Fig. 14. Effect of ellagic acid loaded zinc nanoparticleson grades of vascular and sinusoidal congestion in liver specimen a Significantly different compared with control group, b Significantly different compared with streptozotocin group at (P < 0.05).

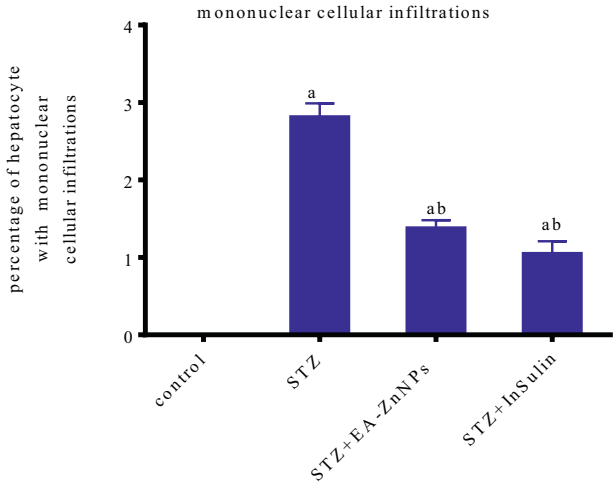

Fig. 15. Effect of ellagic acid loaded zinc nanoparticles on grades of mononuclear cellular infiltrations in liver specimen a. Significantly different compared with control group, b Significantly different compared with streptozotocin group at (P < 0.05).

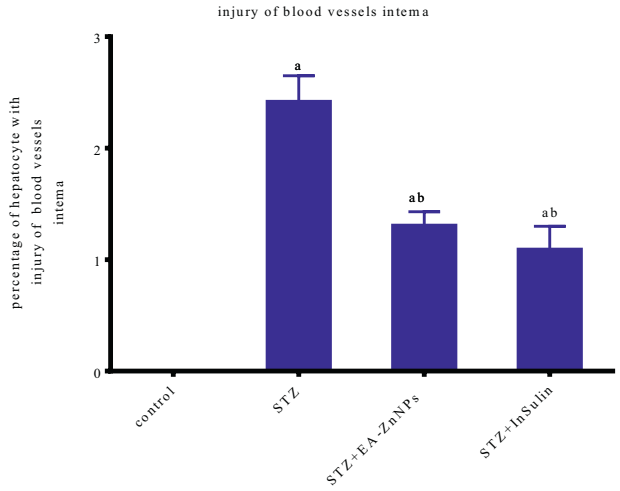

Fig. 16. Effect of ellagic acid loaded zinc nanoparticles on grades of injury of blood vessels interma in liver specimen, a Significantly different compared with control group, b Significantly different compared with streptozotocin group at (P < 0.05).

4. Discussion

Long-term hyperglycemia associated with oxidative damage and inflammation has a role in the development of DC such as neuropathy, retinopathy, nephropathy, cardiovascular disease, and fatty liver disease [42]. DM management and treatment have become a significant concern for researchers and physicians as the number of diabetic patients has grown [43]. The present therapeutic approach to DC remains unsatisfactory, with most medicinal approaches incapable of reversing or even postponing disease development. In this regard, nanomedicine offers new hope in biomedicine used for the treatment of DC due to its adaptability, precision, and intelligence in well-designed nanomaterials. Also, its higher bioavailability and its modulatory potential on hyperglycemia-induced ROS.

The biosynthesized EA-ZnNPs were characterized via FT-IR spectroscopy, Our results showed agreement with [44], that showed the FT-IR procedure was to recognize the interaction between Zn and EA confirming the embodiment of EA in the nanoparticle. The shift at the peak site to Zn++ ion indicates bond formation between zinc and ellagic acid. Ultraviolet-visible (UV/VIS) absorbance spectroscopy for EA-ZnNPs showed peaks almost the same as the UV spectrum of free EA [45].

Our findings are consistent with earlier research showing that TEM for EA-ZnNPs were spherical clusters in shape with relatively narrow particles of average size 29.1 nm, which may be due to the tendency of Zn atoms and EA to merge through hydrogen bond [27]. indicating their low scale, as

the size of nanoparticles is an important factor that significantly influences their biological activity [46].

Streptozotocin, a broad-spectrum antibiotic, has a methyl nitrosourea moiety attached to the deoxy form of glucose that targets the β cells of the pancreatic Langerhans' islets [47]. The pancreatic Langerhans' islets get damaged as a result. Streptozotocin adheres to the glucose transporter 2 receptor, which is widely distributed on the plasma membrane of β cells [48].

In both types of diabetic rats, ROS not only irreversibly induces oxidative modification to proteins, lipids, and DNA. but also promotes leukocyte infiltration, triggers inflammation by controlling NF-κB, and primarily triggers intrinsic (mitochondria-mediated) cell death, which results in cell apoptosis [49,50].

Diagnostic markers of myocardial cell injury include cytosolic enzymes like CK-MB and LDH, which leak into the bloodstream from injured tissues when the cell membrane ruptures or becomes permeable [51]. In the current investigation, the levels of CK-MB and LDH were markedly elevated in the diabetic rats, demonstrating the clear damage that diabetes does to the heart tissue. These results are consistent with previous publications, which found that serum CK-MB and LDH levels increased in STZ diabetic rats, probably due to myocardial infarction [52].

Hyperglycemia and hyperlipidemia, resulting from carbohydrate and lipid metabolic abnormalities, may have a role in the development of cardiac dysfunction in diabetes mellitus [53]. The overproduction of ROS resulting from this metabolic stress in the tissue leads to the development of oxidative stress [54]. Under stressful conditions, ROS causes the polyunsaturated fatty acids to undergo lipid peroxidation, with MDA as the byproduct. Thus, a rise in MDA levels denotes a higher degree of oxidative stress in essential bodily tissues like the brain, liver, heart, and other organs, as well as the red blood cells plasma membrane, caused by a toxicant like STZ [55]. In contrast, the primary characteristic of antioxidant enzymes is their ability to protect the body against oxidative stress by balancing the production of ROS and the antioxidant defense system that results from this stress [56], and the decline in these antioxidant enzymes showed that the antioxidant system had failed, which could lead to hepatic and cardiac damage [57].

Our findings are consistent with earlier research showing that hyperglycemia causes the generation of ROS, simultaneously decreasing the antioxidant enzymes CAT and GPX activities as well as raising the level of lipid peroxidation in the heart and liver [58].

Examining the effects of EA-ZnNPs on the heart, the elevated serum LDH and CK-MB activities associated with diabetic induction were significantly suppressed by EA-ZnNPs administration. This suggests that EA-ZnNPs have good cardioprotective effects in diabetic animals, which can be attributed to their indirect antioxidant action through the induction of endogenous protective enzymes and their direct antioxidant effect through the unique structure of EA, which contains four hydroxyls and two lactone functional groups and can scavenge different types of free radicals, nitrogen reactive species, and ROS, including hydroxyl radicals, peroxyl radicals, NO_2 radicals, and peroxynitrite. In addition, EA may decrease oxidative stress through indirect antioxidant action, such as inhibition of ROS-producing enzymes like myeloperoxidase, lipoxygenase, cyclooxygenase, and xanthine oxidase [59,60]. Moreover, the intrinsic properties of ZnNPs are mostly characterized by their size, composition, crystallinity, and morphology, and reducing the size to the nanoscale can modify their chemical, mechanical, electrical, structural, morphological, and optical properties. These modified features guide EA-ZnNPs to the desired site to interact uniquely with cell biomolecules and thus facilitate the physical transfer of EA-ZnNPs into the inner cellular structures. As a result, ellagic acid and zinc concentrations in the tissue will accumulate leading to high antioxidant and anti-inflammatory effects [61].

Also, Zn plays an inhibitory role on NADPH oxidases (a group of plasma membrane-associated enzymes), which catalyze the transfer of electrons to O_2 generating superoxide, or H_2O_2. In addition the dismutation of O_2 to H_2O_2 is catalyzed by superoxide dismutase (SOD), which contains Cu and Zn. Zn is known to induce the formation of cysteine-rich metallothionein, an excellent scavenger of free radical [62].

Several authors have noted changes in the lipid concentration in the serum of diabetic patients, as well as increases in AST and ALT activities [63]. Significant hepatic tissue membrane damage during diabetes is indicated by the substantial leakage of AST and ALT from the liver cytosol into circulation [64]. Hence, elevated AST and ALT activities in this study could be explained as a consequence of liver cell destruction or changes in membrane permeability implying significant hepatic damage by DM. This finding is consistent with the results indicated by [65].

The liver and some other tissues are involved in the uptake, oxidation, and metabolic conversion of

free fatty acids, as well as the synthesis of cholesterol and phospholipids [66], and the liver is recognized as one of the body's primary metabolic organs, controlling and preserving lipid homeostasis. STZ-induced diabetic rats have been reported to exhibit hypercholesterolemia and hypertriglyceridemia. Overproduction of free fatty acids in STZ-induced diabetes stimulates the liver to convert the overproduction of fatty acids into cholesterol and phospholipids [67]. The elevated amounts of TGs and TC in diabetic rats could be attributed to liver damage from STZ, which acts either directly or indirectly by raising plasma glucose levels [68]. It has been reported that insulin insufficiency in diabetes causes several disruptions in metabolic and regulatory functions, which ultimately cause the accumulation of fat in the liver tissue [67].

The treatment of EA-ZnNPs in our earlier work (under publication) prompted an increase in insulin levels and a drop in glucose levels. Therefore, the reduction in TGs, and cholesterol levels may be dependent on EA-ZnNPs directly protecting the liver and mediating low levels of insulin and high blood glucose. Furthermore, the decrease in TG and cholesterol levels supports the capacity of EA-ZnNPs to enhance lipid metabolism in DM. These results imply that our nanoparticles may help ameliorate cardiovascular problems and fatty liver caused by a disturbance in lipid metabolism that usually developed in DM.

Besides, EA-ZnNPs ameliorated hyperlipidemia can be attributed to suppressing fatty acid synthase, subsequently lowering TGs synthesis. Furthermore, EA-ZnNPs prevented cholesterol synthesis in this study may be by suppressing of the β-hydroxy β-methylglutaryl-CoA reductase (HMGCoAR).

EA-ZnNPs suppress inflammation by downregulating NF-κB and activating anti-inflammatory cytokine IL-10 and this may be through EA. NF-κB is a protein complex that normally lies in the cytoplasm and is linked to another complex called inhibitor of kappa B (IκB). In this state, NF-κB is inactive and cannot perform transcriptional functions. To activate, NF-κB needs to be dissociated from IkB. EA can inhibit the phosphorylation of IkB and subsequent translocation of NF-kB into the nucleus [69], moreover EA possesses anti-inflammatory properties, such as reducing IL-6 and TNF-α, blocking the NF-κB pathway, inhibiting COX-2, and increasing IL-10 [70].

The liver microsections from the STZ-induced diabetic rat group showed mild necrosis and infiltration of hepatocytes (Fig. 12b–d). As previously mentioned, streptozotocin specifically binds to the glucose transporter 2 receptor on the plasma membrane of β cells, and these same receptors are also present on the cell membranes of the liver. Consequently, giving STZ to animal models could also affect the function of the liver [71].

However, after receiving EA-ZnNPs treatment, the observed decline in the serum levels of the above enzymes may be attributed to cell membrane stability and cellular regeneration. These findings support the hepatoprotective role of EA-ZnNPs. Hepatic histoarchitecture was also ameliorated in photomicrographs of liver microsections from STZ-induced diabetic rats treated with EA-ZnNPs (Fig. 12e). EA-ZnNPs also reduced levels of ROS, MDA, downregulated NF-κB and upregulated IL-10. Also, stimulated levels of GPX and CAT in the livers of diabetic rats. These data suggest potent antioxidant and anti-inflammatory effects of EA-ZnNPs.

Our findings proved that cardiac and hepatic protective effect of EA-ZnNPs against STZ induced diabetes was nearly similar to that of insulin, so we recommend using of EA-ZnNPs orally as a step before shifting to s/c injection of insulin or used together with lower insulin dose.

5. Conclusion

The application of EA-ZnNPs in treating DM-related hepatic and cardiac dysfunctions notably reduced oxidative stress by improving the antioxidant defense capacity, restored heart and liver function, and preserved the liver architecture in STZ-induced DM in rats.

Ethics approval

This study was conducted according to the standards of the Research Ethics Committee (Ph. D/67). Faculty of Veterinary Medicine, Mansoura University, Egypt.

Availability of data and materials

The authors confirm that the data supporting the findings of this study is available within the article.

Author contributions

F.E.S.: methodology, formal analysis, data curation, writing original draft, review, and editing; A.D.A., H.B.H., A.F. and G.R.M.E.: conceptualization, validation, visualization, editing the final draft, supervision, and reviewing; G.R.M.E.: final review and preparing the manuscript for publication. All authors read and approved the final manuscript.

Funding

The present study was a self-funding study.

Conflicts of interest

There are not competing interests.

Acknowledgements

This project did not receive any grant from any funding agency.

References

[1] Rawshani A, Sattar N, Franzén S, Rawshani A, Hattersley AT, Svensson A-M, et al. Excess mortality and cardiovascular disease in young adults with type 1 diabetes in relation to age at onset: a nationwide, register-based cohort study. Lancet 2018;392(10146):477−86.
[2] Nabi R, Alvi SS, Shah A, Chaturvedi CP, Faisal M, Alatar AA, et al. Ezetimibe attenuates experimental diabetes and renal pathologies via targeting the advanced glycation, oxidative stress and AGE-RAGE signalling in rats. Arch Physiol Biochem 2023;129(4):831−46.
[3] Huang D, Refaat M, Mohammedi K, Jayyousi A, Al Suwaidi J, Khalil CA. Macrovascular complications in patients with diabetes and prediabetes. BioMed Res Int 2017; 2017:7839101.
[4] Dal Canto E, Ceriello A, Rydén L, Ferrini M, Hansen TB, Schnell O, et al. Diabetes as a cardiovascular risk factor: an overview of global trends of macro and micro vascular complications. Eur J Preventive Cardiol 2019;26(2_suppl): 25−32.
[5] Colombo A, Meroni CA, Cipolla CM, Cardinale D. Managing cardiotoxicity of chemotherapy. Curr Treat Options Cardiovasc Med 2013;15:410−24.
[6] Alicic RZ, Rooney MT, Tuttle KR. Diabetic kidney disease: challenges, progress, and possibilities. Clin J Am Soc Nephrol 2017;12:2032.
[7] Dey A, Swaminathan K. Hyperglycemia-induced mitochondrial alterations in liver. Life Sci 2010;87:197−214.
[8] Francés DE, Ronco MT, Monti JA, Ingaramo PI, Pisani GB, Parody JP, et al. Hyperglycemia induces apoptosis in rat liver through the increase of hydroxyl radical: new insights into the insulin effect. J Endocrinol 2010;205(2):187.
[9] Natesan V, Kim S-J. The trend of organic based nanoparticles in the treatment of diabetes and its perspectives. Biomol Therap 2023;31:16.
[10] Beard JR, Officer A, De Carvalho IA, Sadana R, Pot AM, Michel J-P, et al. The World report on ageing and health: a policy framework for healthy ageing. Lancet 2016;387(10033): 2145−54.
[11] Singla R, Guliani A, Kumari A, Yadav SK. Metallic nanoparticles, toxicity issues and applications in medicine. In: Nanoscale materials in targeted drug delivery, theragnosis and tissue regeneration; 2016. p. 41−80.
[12] Arulselvan P, Subramanian SP. Beneficial effects of Murraya koenigii leaves on antioxidant defense system and ultra structural changes of pancreatic β-cells in experimental diabetes in rats. Chem Biol Interact 2007;165:155−64.
[13] Strati A, Papoutsi Z, Lianidou E, Moutsatsou P. Effect of ellagic acid on the expression of human telomerase reverse transcriptase (hTERT) α+ β+ transcript in estrogen receptor-positive MCF-7 breast cancer cells. Clin Biochem 2009;42(13-14):1358−62.
[14] Hussein-Al-Ali SH, Hasan S, Balavandy SK, Abidin ZZ, Umar Kura A, Fakurazi S, et al. The in vitro therapeutic activity of ellagic acid-alginate-silver nanoparticles on breast cancer cells (MCF-7) and normal fibroblast cells (3T3). Sci Adv Mater 2016;8(3):545−53.
[15] Hussein MZ, Ali SHA, Zainal Z, Hakim MN. Development of antiproliferative nanohybrid compound with controlled release property using ellagic acid as the active agent. Int J Nanomed 2011:1373−83.
[16] Farbood Y, Rashno M, Ghaderi S, Khoshnam SE, Sarkaki A, Rashidi K, et al. Ellagic acid protects against diabetes-associated behavioral deficits in rats: possible involved mechanisms. Life Sci 2019;225:8−19.
[17] Ceci C, Graziani G, Faraoni I, Cacciotti I. Strategies to improve ellagic acid bioavailability: from natural or semi-synthetic derivatives to nanotechnological approaches based on innovative carriers. Nanotechnology 2020;31:382001.
[18] Harakeh S, Almuhayawi M, Jaouni SA, Almasaudi S, Hassan S, Amri TA, et al. Antidiabetic effects of novel ellagic acid nanoformulation: insulin-secreting and anti-apoptosis effects. Saudi J Biol Sci 2020;27(12):3474−80.
[19] Kaur H, Ghosh S, Kumar P, Basu B, Nagpal K. Ellagic acid-loaded, tween 80-coated, chitosan nanoparticles as a promising therapeutic approach against breast cancer: in-vitro and in-vivo study. Life Sci 2021;284:119927.
[20] Bala I, Bhardwaj V, Hariharan S, Vo Kharade S, Roy N, Ravi Kumar MNV. Sustained release nanoparticulate formulation containing antioxidant-ellagic acid as potential prophylaxis system for oral administration. J Drug Target 2006;14(1): 27−34.
[21] McCall KA, Huang C-C, Fierke CA. Function and mechanism of zinc metalloenzymes. J Nutr 2000;130:1437S−46S.
[22] Chausmer AB. Zinc, insulin and diabetes. J Am Coll Nutr 1998;17:109−15.
[23] Qi Y, Zhang Z, Liu S, Aluo Z, Zhang L, Yu L, et al. Zinc supplementation alleviates lipid and glucose metabolic disorders induced by a high-fat diet. J Agric Food Chem 2020; 68(18):5189−200.
[24] Szkudelski T. The mechanism of alloxan and streptozotocin action in B cells of the rat pancreas. Physiol Res 2001;50: 537−46.
[25] Moreno-Álvarez S, Martínez-Castañón GA, Niño-Martínez N, Reyes-Macías JF, Patiño-Marín N, Loyola-Rodríguez JP, et al. Preparation and bactericide activity of gallic acid stabilized gold nanoparticles. J Nanoparticle Res 2010;12:2741−6.
[26] Litchfield JJ, Wilcoxon F. A simplified method of evaluating dose-effect experiments. J Pharmacol Exp Therap 1949;96: 99−113.
[27] El Barky AR, Mohamed TM, Ali EMM. Detoxifying and antioxidant effect of ellagic acid nano particles in rats intoxicated with sodium nitrites. Applied Biol Chem 2020;63: 1−16.
[28] Yavuz O, Cam M, Bukan N, Guven A, Silan F. Protective effect of melatonin on β-cell damage in streptozotocin-induced diabetes in rats. Acta Histochem 2003;105(3):261−6.
[29] Hussein SA, Hassanein MRR, Awadalla MA. The ameliorative effect of proanthocyanidinsagainst streptozotocin induced diabetic nephropathy in rats. Benha Vet Med J 2018; 34:42−56.
[30] Richmond W. Proceedings: the development of an enzymic technique for the assay of cholesterol in biological fluids. Clin Sci Mol Med 1974;46:6P−7P.
[31] Fossati P, Prencipe L. Serum triglycerides determined colorimetrically with an enzyme that produces hydrogen peroxide. Clin Chem 1982;28:2077−80.
[32] Reitman S, Frankel S. A colorimetric method for the determination of serum glutamic oxalacetic and glutamic pyruvic transaminases. Am J Clin Pathol 1957;28:56−63.
[33] Rechsteiner MC. Drosophila lactate dehydrogenase: partial purification and characterization. J Insect Physiol 1970;16: 957−77.
[34] Mesbah L, Soraya B, Narimane S, Jean PF. Protective effect of flavonides against the toxicity of vinblastine cyclophosphamide and paracetamol by inhibition of lipid−peroxydation and increase of liver glutathione. Haematol 2004;7(1):59−67.

[35] Flohé L, Günzler WA. [12] Assays of glutathione peroxidase. In: Methods in enzymology. 105. Academic Press; 1984. p. 114−20.
[36] Aebi H. [13] Catalase in vitro. In: Methods in enzymology. 105. Academic press; 1984. p. 121−6.
[37] Yuan JS, Ann R, Chen F, Stewart CN. Statistical analysis of real-time PCR data. BMC Bioinf 2006;7:1−12.
[38] Banni M, Messaoudi I, Said L, El Heni J, Kerkeni A, Said K. Metallothionein gene expression in liver of rats exposed to cadmium and supplemented with zinc and selenium. Arch Environ Contam Toxicol 2010;59(3):513−9.
[39] Shynlova O, Dorogin A, Li Y, Lye S. Inhibition of infection-mediated preterm birth by administration of broad spectrum chemokine inhibitor in mice. J Cell Mol Med 2014;18(9): 1816−29.
[40] Kermanian F, Soleimani M, Ebrahimzadeh A, Haghir H, Mehdizadeh M. Effects of adenosine A2a receptor agonist and antagonist on hippocampal nuclear factor-kB expression preceded by MDMA toxicity. Metab Brain Dis 2013;28:45−52.
[41] Abu EHW, Soufy H, EL-Shemy A, Fotouh A, Nasr MN, Dessouky MI. Prophylactic Effect of Oregano in Chickens Experimentally Infected with Avian Pathogenic Escherichia coli O27 with Special Reference to Hematology, Serum Biochemistry, and Histopathology of Vital Organs. Egypt J Chem 2022;65(6):269−82.
[42] Volpe CMO, Villar-Delfino PH, Dos Anjos PMF, Nogueira-Machado JA. Cellular death, reactive oxygen species (ROS) and diabetic complications. Cell Death Dis 2018;9(2):119.
[43] Sen S, Chakraborty R. EDITORIAL (thematic issue: treatment and diagnosis of diabetes mellitus and its complication: advanced approaches). Mini Rev Med Chem 2015;15:1132−3.
[44] Arulmozhi V, Pandian K, Mirunalini S. Ellagic acid encapsulated chitosan nanoparticles for drug delivery system in human oral cancer cell line (KB). Colloids Surf B Biointerfaces 2013;110:313−20.
[45] Chittrarasu M. Biosynthesis and physicochemical characterisation of zinc oxide nanoparticles.
[46] Shin SW, Song IH, Um SH. Role of physicochemical properties in nanoparticle toxicity. Nanomaterials 2015;5:1351−65.
[47] Johansson EB, Tjälve H. The distribution of [14 C] dimethylnitrosamine in mice. Autoradiographic studies in mice with inhibited and noninhibited dimethylnitrosamine metabolism and a comparison with the distribution of [14 C] formaldehyde. Toxicol Appl Pharmacol 1978;45:565−75.
[48] Lenzen S. The mechanisms of alloxan-and streptozotocin-induced diabetes. Diabetologia 2008;51:216−26.
[49] Rodríguez V, Plavnik L, de Talamoni NT. Naringin attenuates liver damage in streptozotocin-induced diabetic rats. Biomed Pharmacother 2018;105:95−102.
[50] Kawai T, Kayama K, Tatsumi S, Akter S, Miyawaki N, Okochi Y, et al. Regulation of hepatic oxidative stress by voltage-gated proton channels (Hv1/VSOP) in Kupffer cells and its potential relationship with glucose metabolism. FASEB J 2020;34(12):15805−21.
[51] Farvin KS, Anandan R, Hari Senthil Kumar S, Shiny KS, Sankar TV, Thankappan TK, et al. Effect of squalene on tissue defense system in isoproterenol-induced myocardial infarction in rats. Pharmacol Res 2004;50(3):231−6.
[52] Farshid AA, Tamaddonfard E, Moradi-Arzeloo M, Mirzakhani N. The effects of crocin, insulin and their co-administration on the heart function and pathology in streptozotocin-induced diabetic rats. Avicenna J Phytomed 2016;6(6):658.
[53] Rodriguez-Araujo G, Nakagami H. Pathophysiology of cardiovascular disease in diabetes mellitus. Cardiovasc Endocrinol Metab 2018;7:4.
[54] Rodrigues B, Cam MC, McNeill JH. Metabolic disturbances in diabetic cardiomyopathy. Mol Cell Biochem 1998;180: 53−7.
[55] Balakumar P, Singh M. The possible role of caspase-3 in pathological and physiological cardiac hypertrophy in rats. Basic Clin Pharmacol Toxicol 2006;99:418−24.
[56] Ye G, Metreveli NS, Donthi RV, Xia S, Xu M, Carlson EC, et al. Catalase protects cardiomyocyte function in models of type 1 and type 2 diabetes. Diabetes 2004;53(5):1336−43.
[57] Lubrano V, Balzan S. Enzymatic antioxidant system in vascular inflammation and coronary artery disease. World J Exp Med 2015;5:218.
[58] Papachristoforou E, Lambadiari V, Maratou E, Makrilakis K. Association of glycemic indices (hyperglycemia, glucose variability, and hypoglycemia) with oxidative stress and diabetic complications. J Diabetes Res 2020;2020(1):7489795.
[59] Nugroho A, Rhim T-J, Choi M-Y, Choi JS, Kim Y-C, Kim M-S, et al. Simultaneous analysis and peroxynitrite-scavenging activity of galloylated flavonoid glycosides and ellagic acid in Euphorbia supina. Arch Pharm Res 2014;37:890−8.
[60] Cozzi R, Ricordy R, Bartolini F, Ramadori L, Perticone P, De Salvia R. Taurine and ellagic acid: two differently-acting natural antioxidants. Environ Mol Mutagen 1995;26(3):248−54.
[61] Rasmussen JW, Martinez E, Louka P, Wingett DG. Zinc oxide nanoparticles for selective destruction of tumor cells and potential for drug delivery applications. Expet Opin Drug Deliv 2010;7(9):1063−77.
[62] Prasad AS. Zinc in human health: effect of zinc on immune cells. Mol Med 2008;14:353−7.
[63] Ali F, Naqvi SAS, Bismillah M, Wajid N. Comparative analysis of biochemical parameters in diabetic and non-diabetic acute myocardial infarction patients. Indian Heart J 2016;68(3):325−31.
[64] Contreras-Zentella ML, Hernández-Muñoz R. Is liver enzyme release really associated with cell necrosis induced by oxidant stress? Oxid Med Cell Longev 2016;2016:3529149.
[65] Ghanbari E, Nejati V, Khazaei M. Improvement in serum biochemical alterations and oxidative stress of liver and pancreas following use of royal jelly in streptozotocin-induced diabetic rats. Cell J (Yakhteh) 2016;18:362.
[66] Feingold KR. Introduction to lipids and lipoproteins. 2015.
[67] Saravanan G, Ponmurugan P. Ameliorative potential of S-allylcysteine: effect on lipid profile and changes in tissue fatty acid composition in experimental diabetes. Exp Toxicol Pathol 2012;64:639−44.
[68] Li S, Chen H, Wang J, Wang X, Hu B, Lv F. Involvement of the PI3K/Akt signal pathway in the hypoglycemic effects of tea polysaccharides on diabetic mice. Int J Biol Macromol 2015;81:967−74.
[69] Sarkar S, Siddiqui AA, Mazumder S, De R, Saha SJ, Banerjee C, et al. Ellagic acid, a dietary polyphenol, inhibits tautomerase activity of human macrophage migration inhibitory factor and its pro-inflammatory responses in human peripheral blood mononuclear cells. J Agric Food Chem 2015;63(20):4988−98.
[70] Kaur R, Mehan S, Khanna D, Kalra S. Polyphenol ellagic acid−targeting to brain: a hidden treasure. Int J Neurol Res 2015;1(3):141−52.
[71] Bouwens L, Rooman I. Regulation of pancreatic beta-cell mass. Physiol Rev 2005;85:1255−70.